Simulation Study and Sensitivity Analysis on DOA Estimation Using ESPRIT Algorithm

H. K. Hwang, Zekeriya Aliyazicioglu, Alfred Tsz Yin Lok

***Abstract*—An array antenna system with innovative signal processing can enhance the resolution of a signal direction of arrival (DOA) estimation. The performance of DOA using an estimation signal parameter via a rotational invariant technique (ESPRIT) is investigated in this paper. The DOA angles are derived from the auto-correlation and cross-correlation matrices. Three matrix estimation methods, (1) temporal averaging, (2) spatial smoothing, (3) temporal averaging and spatial smoothing are used to evaluate the performance. Extensive computer simulations are used to demonstrate the performance of the processing algorithms. The DOA performance as a function of signal to noise ratio (SNR), number of snapshots and effect of spatial smoothing are discussed. The position of array antenna elements may deviate from the ideal location. The imprecise element position will increase the DOA estimation variance. Sensitivity analysis due to non-ideal element position is also discussed in this paper**

***Index Terms*—DOA estimation, array antenna, ESPRIT algorithm, advanced signal processing.**

I. Introduction

Accurately estimating the direction of arrival (DOA) has many important applications in communication and radar systems. Using the conventional fixed antenna, the resolution of DOA is limited by the antenna mainlobe beamwidth. Using an array antenna and advanced signal processing techniques, the DOA estimation variance can be greatly reduced.

Two important classes of signal processing techniques are the model based approach and the eigen-analysis method [1]. The model based method assumes that the received data is modeled as the output of a linear shift invariant system. The DOA information can be obtained indirectly from the estimated model parameters. Several eigen-analysis methods such as multiple signal classification (MUSIC) [2], root MUSIC [3,4], polynomial root intersection for multi-dimensional estimation (PRIME) [5,6] have been investigated by many authors. This paper studies DOA finding using an estimation signal parameter via a rotational invariant technique (ESPRIT) [7]. Two different array antennas are used in this simulation study. In this paper DOA performance is discussed as a function of signal to noise ratio (SNR), number of snapshots and the effect of spatial smoothing.

Sample time can be precisely defined in a digital processor. Thus, applying the ESPRIT [8-12] method in time domain analysis provides an excellent result. However, it is relatively difficult to maintain the precise array element position, and the estimation variance of ESPRIT in spatial application will be increased. This paper provides statistical analysis of DOA estimation resulting from an imprecise array element position. Using the spatial smoothing method, an array with a large number of elements tends to average out the imprecise element position effect. The effects of the number of array elements, rank of matrices, number of snapshots, and signal to noise ratio (SNR) to the DOA performance are studied in this paper.

Manuscript received January 12, 2010. This work was supported in part by the Raytheon Space and Airborne Systems.

H. K. Hwang is with the Electrical and Computer Engineering Department, California State Polytechnic University, Pomona, CA 91768 USA (phone: 909-869-2539; fax: 909-869-4687; e-mail: hkhwang@csupomona.edu).

Z. Aliyazicioglu is with the Electrical and Computer Engineering Department, California State Polytechnic University, Pomona, CA 91768 USA (phone: 909-869-3667; fax: 909-869-4687; e-mail: zaliyazici@csupomona.edu).

Alfred Tsz Yin Lok is a graduate student at the Electrical and Computer Engineering Department, California State Polytechnic University, Pomona, CA 91768 (e-mail: loktszyin@hotmail.com).

II. Narrowband Signal Modeling

Two different array antennas are considered in this paper, a square array with 9 elements and a honeycomb array with 19 elements. Array elements are uniformly placed on an x-y plane as shown in Figure 1. The inter-element spacing d equals half of the signal wavelength.

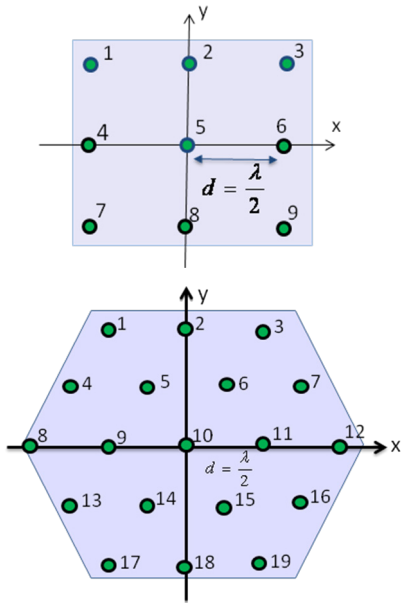

Figure 1 Two Dimensional Arrays with 9 and 19 Elements

Assume a narrowband signal impinging on the array from an elevation angle θ and azimuth angle ϕ as shown in Figure 2. The narrowband signal is defined by the signal bandwidth and is a small fraction of c/D where c is the speed of light and D is the diameter of the array antenna. The narrowband signal waveform $s_c(t)$ can be expressed as

$$s_c(t) = m(t)\, e^{j2\pi f_c t} \tag{1}$$

where m(t) is the baseband waveform and f_c is the center frequency of the narrowband signal.

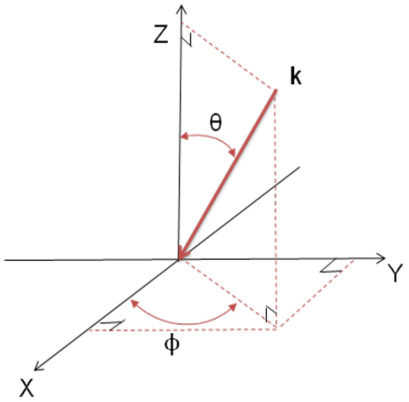

Figure 2 Coordinate of array system and signal direction

Let $s_c(t)$ be the signal at the reference point. Without loss of generality, this reference point is assigned to the sensor at the center of the array, which is sensor 5 for the 9 element sensor and sensor 10 for the 19 element sensor array. Due to the propagation path difference, the signal at the i^{th} sensor $s_i(t)$ is related to the reference $s_c(t)$ by

$$s_i(t) = s_c(t - \tau_i) = m(t- \tau_i)\, e^{j2\pi f_c (t-\tau_i)} \tag{2}$$

where the propagation delay time of the i^{th} element τ_i is $\tau_i = -\sin\theta(x_i\cos\phi + y_i\sin\phi)/c$. For the narrowband signal, $m(t- \tau_i) \approx m(t)$, thus

$$s_i(t) = m(t)\, e^{j2\pi f_c t}\ \ e^{-j2\pi f_c \tau_i} = s_c(t)\, e^{j\beta_i} \tag{3}$$

where the electrical angle of the i^{th} element β_i is

$$\beta_i = \frac{2\pi}{\lambda}\sin\theta(x_i\cos\phi + y_i\sin\phi) \tag{4}$$

where (x_i, y_i) are the coordinates of the i^{th} element.

If there are L signals impinging on this array, assume the k^{th} signal at the reference sensor is $s_{c,k}(t)$. For the narrowband waveform, this signal at the i^{th} sensor is related to the reference signal $s_{c,k}(t)$ by a electrical angle $\beta_{i,k}$ as given by

$$s_{i,k}(t) = s_{c,k}(t)\, e^{j\beta_{i,k}},\ i = 1, \ldots, M \text{ and } k = 1, \ldots, L \tag{5}$$

The continuous sensor output waveform may be sampled at the sampling rate. Define the received data vector at sample n as $\mathbf{y}(n) = [y_1(n), y_2(n), \ldots, y_M(n)]^T$, where $y_i(n)$, i = 1, 2, … , M is the signal at i^{th} sensor and the reference sensor $y_c(n)$ is $y_5(n)$ for the 9 element sensor and $y_{10}(n)$ for the 19 element sensor array. The received data vector **y**(n) consists of a signal component **s**(n) and a noise component **w**(n),

$$\mathbf{y}(n) = \mathbf{s}(n) + \mathbf{w}(n) \tag{5}$$

where

$$\mathbf{s}(n) = \sum_{k=1}^{L} s_{c,k}(n)\mathbf{v}_k \tag{6}$$

where $\mathbf{v}_k$ is the array manifold vector of k^{th} signal and $e^{j\beta_{i,k}}$ is the phase factor of i^{th} element due to k^{th} signal, and $w_i(n)$, i = 1, 2, … , M are independent white noise sequences.

$$\mathbf{v}_k = \begin{bmatrix} 1 \\ e^{j\beta_{2,k}} \\ \vdots \\ e^{j\beta_{M,k}} \end{bmatrix} \tag{7}$$

$$\mathbf{w}(n) = \begin{bmatrix} w_1(n) \\ w_2(n) \\ \vdots \\ w_M(n) \end{bmatrix} \tag{8}$$

III. ESPRIT Algorithm

A brief description of the ESPRIT algorithm is presented in this section. Two different antennas investigated in this study are (a) a 9 element square array antenna and (b) a19 element honeycomb array antenna. Their configurations are shown in Figure 1(a) and 1(b) respectively. The inter-element spacing is $d = \lambda/2$, where λ is the signal wavelength.

Equation (4) shows that the signal DOA angles (θ, ϕ) are related to the electrical angle β. The ESPRIT algorithm derives the DOA angles from the phase factor β. Determining two angles (θ, ϕ) requires two different phase factors. Two independent phase factors can be derived from two independent position shifts. A brief description of ESPRIT using a 9 element square array is as follows:

The waveform **y** received by the subset consists of elements (1, 2, 4, 5) as shown in Figure 3 and can be expressed as:

$$\mathbf{y}(n) = s_5(n)\mathbf{s} + [w_1(n), w_2(n), w_4(n), w_5(n)]^T \tag{9}$$

where $s_5(n)$ is the signal received by center element, $\mathbf{s} = [e^{j\beta_1}, e^{j\beta_2}, e^{j\beta_4}, 1]^T$, and $w_k(n)$ k = 1, 2, 4, 5 are the white noise received by the elements of this subset. The correlation matrix $\mathbf{R}_{yy}$ of this subset is

$$\mathbf{R}_{yy} = E[\mathbf{y}\mathbf{y}^H] = \sigma_s^2\, \mathbf{s}\mathbf{s}^H + \sigma_w^2\, \mathbf{I} \tag{10}$$

where σ_s^2 and σ_w^2 are the variance of signal and noise respectively.

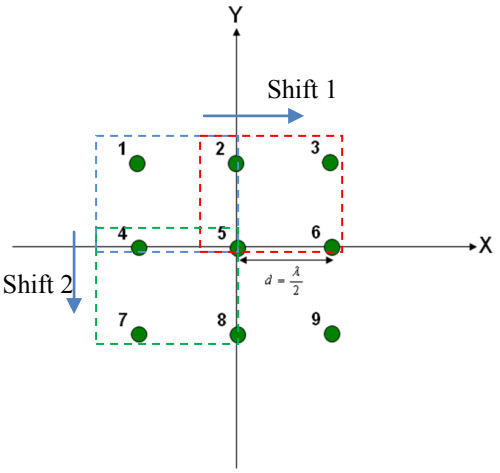

Figure 3 subset selections on 9 Element Square Array

Shifting this subset horizontally to the right forms a new subset consisting of elements (2, 3, 5, 6). The received waveform of this new subset **z**(n) is

$$\mathbf{z}(n) = e^{j\beta_6} s_5(n)\left[e^{j\beta_1}, e^{j\beta_2}, e^{j\beta_4}, 1\right]^T + \left[w_2(n), w_3(n), w_5(n), w_6(n)\right]^T \quad (11)$$

The cross correlation matrix $\mathbf{R}_{yz}$ is

$$\mathbf{R}_{yz} = E[\mathbf{y}\mathbf{z}^H] = \sigma_s^2 e^{j\beta_6} \mathbf{s}\mathbf{s}^H + \sigma_w^2 \mathbf{Q} \quad (12)$$

where $\mathbf{Q} = \begin{bmatrix} 0 & 0 & 0 & 0 \\ 1 & 0 & 0 & 0 \\ 0 & 0 & 0 & 0 \\ 0 & 0 & 1 & 0 \end{bmatrix}$

Arranging the eigenvalues of matrix $\mathbf{R}_{yy}$ λ_1, λ_2, λ_3, λ_4 in descending order, the noise variance σ_w^2 can be estimated by the following equation.

$$\sigma_w^2 = (\lambda_2 + \lambda_3 + \lambda_4)/3 \quad (13)$$

Define matrices $\mathbf{C}_{yy}$ and $\mathbf{C}_{yz}$ as

$$\mathbf{C}_{yy} = \mathbf{R}_{yy} - \sigma_w^2 \mathbf{I} = \sigma_s^2 \mathbf{s}\mathbf{s}^H \quad (14)$$

$$\mathbf{C}_{yz} = \mathbf{R}_{yz} - \sigma_w^2 \mathbf{Q} = \sigma_s^2 e^{j\beta_6} \mathbf{s}\mathbf{s}^H \quad (15)$$

Then $\mathbf{C}_{yy} - \lambda\mathbf{C}_{yz} = \sigma_s^2 (1 - \lambda e^{j\beta_6})\mathbf{s}\mathbf{s}^H$, thus $\lambda = e^{-j\beta_6}$ is one of the roots of $\det(\mathbf{C}_{yy} - \lambda \mathbf{C}_{yz})$. One phase factor β_6 can be obtained by finding the root of $\det(\mathbf{C}_{yy} - \lambda \mathbf{C}_{yz})$ closest to the unit circle.

Forming subset (4, 5, 7, 8) by shifting the subset (1, 2, 4, 5) down by d, the second independent phase factor can be obtained. The received data vector of this subset **v** is:

$$\mathbf{v}(n) = e^{j\beta_8} s_5(n)\left[e^{j\beta_1}, e^{j\beta_2}, e^{j\beta_4}, 1\right]^T + \left[w_4(n), w_5(n), w_7(n), w_8(n)\right]^T \quad (16)$$

The cross correlation matrix $\mathbf{R}_{yv}$ is

$$\mathbf{R}_{yv} = E[\mathbf{y}\mathbf{v}^H] = \sigma_s^2 e^{j\beta_8} \mathbf{s}\mathbf{s}^H + \sigma_w^2 \mathbf{Q}_1 \quad (17)$$

where $\mathbf{Q}_1 = \begin{bmatrix} 0 & 0 & 0 & 0 \\ 0 & 0 & 0 & 0 \\ 1 & 0 & 0 & 0 \\ 0 & 1 & 0 & 0 \end{bmatrix}$

Define matrices $\mathbf{C}_{yy}$ and $\mathbf{C}_{yv}$ as:

$$\mathbf{C}_{yy} = \mathbf{R}_{yy} - \sigma_w^2 \mathbf{I} = \sigma_s^2 \mathbf{s}\mathbf{s}^H \quad (18)$$

$$\mathbf{C}_{yv} = \mathbf{R}_{yv} - \sigma_w^2 \mathbf{Q}_1 = \sigma_s^2 e^{j\beta_8} \mathbf{s}\mathbf{s}^H \quad (19)$$

Then $\mathbf{C}_{yy} - \lambda\mathbf{C}_{yv} = \sigma_s^2 (1 - \lambda e^{j\beta_8})\mathbf{s}\mathbf{s}^H$, thus $\lambda = e^{-j\beta_8}$ is one of the roots of $\det(\mathbf{C}_{yy} - \lambda \mathbf{C}_{yv})$. The second phase factor β_8 can be obtained by finding the root of $\det(\mathbf{C}_{yy} - \lambda \mathbf{C}_{yv})$ closest to the unit circle.

Since $\beta_6 = \pi\sin\theta\cos\phi$, $\beta_8 = -\pi\sin\theta\sin\phi$, DOA information can be obtained by solving $e^{j\pi\sin\theta\cos\phi} = r_1 = e^{j\alpha_1}$ where r_1 is the root of $\det(\mathbf{C}_{yy} - \lambda \mathbf{C}_{yz})$ closest to unit circle and $e^{-j\pi\sin\theta\sin\phi} = r_2 = e^{j\alpha_2}$ where r_2 is the root of $\det(\mathbf{C}_{yy} - \lambda \mathbf{C}_{yv})$ closest to unit circle.

$$\pi\sin\theta\cos\phi = \alpha_1 \quad (20)$$

$$-\pi\sin\theta\sin\phi = \alpha_2 \quad (21)$$

The azimuth and elevation angles can be found from the following equations.

$$\phi = \tan^{-1}(-\alpha_2/\alpha_1) \quad (22)$$

$$\theta = \sin^{-1}(\alpha_1/\pi\cos\phi) \quad (23)$$

DOA information using the 19 element honeycomb array can be obtained in similar manner.

IV. Matrix Estimation

Section 3 shows that the DOA angles are derived from the auto-correlation and cross-correlation matrices. DOA performance depends on the accurate estimation of matrices $\mathbf{R}_{yy}$, $\mathbf{R}_{yz}$, $\mathbf{R}_{yv}$. Elements of matrices are estimated from the received data y(n) = s(n) + w(n) where s(n) and w(n) are the signal and white noise of the received data. Three matrix estimation methods, (1) temporal averaging, (2) spatial smoothing, (3) temporal averaging and spatial smoothing, are described in this section[13].

A. Temporal Averaging Method

This method estimates the matrix element r_{ij} by averaging the products of data received by the i^{th} and j^{th} elements over N snapshots according to the following equation:

$$r_{ij} = \frac{1}{N}\sum_{n=1}^{N} y_i(n)y_j^*(n) \tag{24}$$

B. Spatial Smoothing Method

Since the number of elements in the array is larger than the size of the subset, instead of discarding the data from elements outside of the subset, those data can be used to improve the estimation of r_{ij}. For example, elements of the correlation matrix of square array for subset (1, 2, 4, 5) are computed from the following equations.

$$r_{11}(n) = r_{22} = r_{44} = r_{55} = \frac{1}{9}\sum_{i=1}^{9} y_i(n)y_i^*(n) \tag{25}$$

$$r_{12}(n) = \frac{1}{6}\left[y_1(n)y_2^*(n) + y_2(n)y_3^*(n) + y_4(n)y_5^*(n) + y_5(n)y_6^*(n) + y_7(n)y_8^*(n) + y_8(n)y_9^*(n)\right] \tag{26}$$

$$r_{14}(n) = \frac{1}{6}\left[y_1(n)y_4^*(n) + y_2(n)y_5^*(n) + y_3(n)y_6^*(n) + y_4(n)y_7^*(n) + y_5(n)y_8^*(n) + y_6(n)y_9^*(n)\right] \tag{27}$$

$$r_{15}(n) = \frac{1}{4}\left[y_1(n)y_5^*(n) + y_2(n)y_6^*(n) + y_4(n)y_8^*(n) + y_5(n)y_9^*(n)\right] \tag{28}$$

$$r_{24}(n) = \frac{1}{4}\left[y_2(n)y_4^*(n) + y_3(n)y_5^*(n) + y_5(n)y_7^*(n) + y_6(n)y_8^*(n)\right] \tag{29}$$

$$r_{25}(n) = r_{14}(n) \tag{30}$$

$$r_{45}(n) = r_{12}(n) \tag{31}$$

Elements of the cross-correlation matrices can be computed in a similar manner.

This method estimates the matrix element based on a single snapshot. A good estimation would require an array with a large number of elements. Thus, the 19 element honeycomb array would produce a much better spatial smoothing than the 9 element square array. Elements of the cross-correlation matrices can be computed in a similar manner.

C. Temporal Averaging and Spatial Smoothing Method

This method combines spatial smoothing and temporal averaging. After estimating the matrix elements $r_{ij}(n)$ from spatial smoothing, an estimated r_{ij} is obtained by further averaging over N snapshots according to the following equation.

$$r_{ij} = \frac{1}{N}\sum_{n=1}^{N} r_{ij}(n) \tag{32}$$

V. Simulation Results

Assume a tone signal impinging the array from azimuth angle $\phi = 60°$, and elevation angle $\theta = 30°$. The signal to noise ratio SNR = 10 dB. DOA estimation is done using a 9 element square array and generating two independent equations by shifting subset (1, 2, 4, 5) to subset (2, 3, 5, 6) and subset (4, 5, 7, 8) as shown in Figure 3.

Figure 4(a) shows the scatter plot based on 1000 independent simulations using the 9 element square array. The estimated 4×4 matrices are obtained by temporal averaging over only 32 snapshots. Most of the data points are centered on the true signal direction (30°, 60°). There are also points scattered over the other angles. With temporal averaging and spatial smoothing, Figure 4(b) shows an improved scatter plot where most of the data points are concentrated on (30°, 60°). The averaged estimated angle errors for (a) and (b) are 11.84° and 2.19°, respectively. The estimated angle error ε is computed by the following equation.

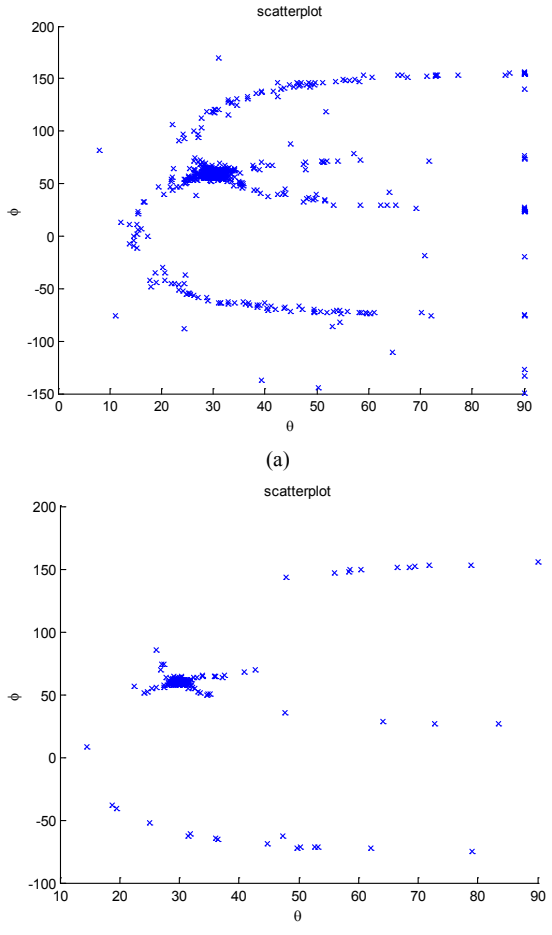

Figure 4 Scatter Plots Based on 1000 Independent Simulations

A 19 element honeycomb array was used and with two independent equations generated by shifting subset (1, 2, 4, 5) to subset (2, 3, 5, 6) and subset (4, 5, 8, 9) is shown in Figure 5.

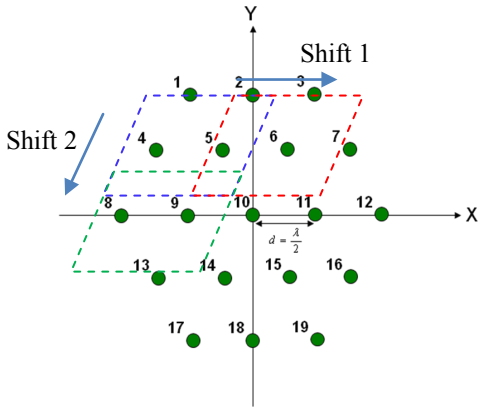

Figure 5 Subset selections on 19 Element Square Array

Figure 6 shows the scatter plots using a 19 element honeycomb array and 4×4 matrices. Figure 6(a) shows the scatter plot of 1000 independent simulations assuming SNR = 10 dB using temporal averaging over 32 snapshots. The result of the combination of temporal averaging and spatial smoothing is shown in Figure 6(b). The estimated angle errors are 12.98° and 0.97° for (a) and (b) respectively. Comparing Figures 4 and 6, the 19 element honeycomb array provides much better performance with spatial smoothing.

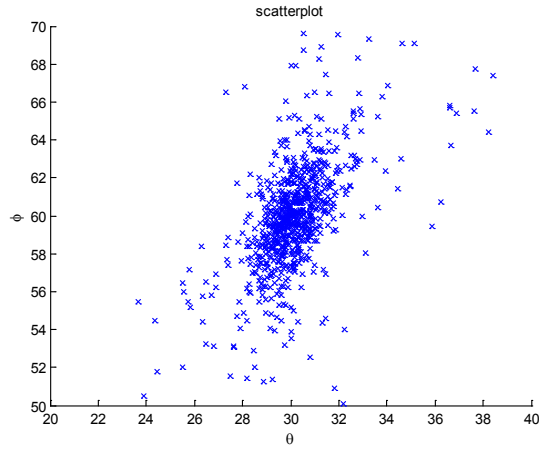

(a)

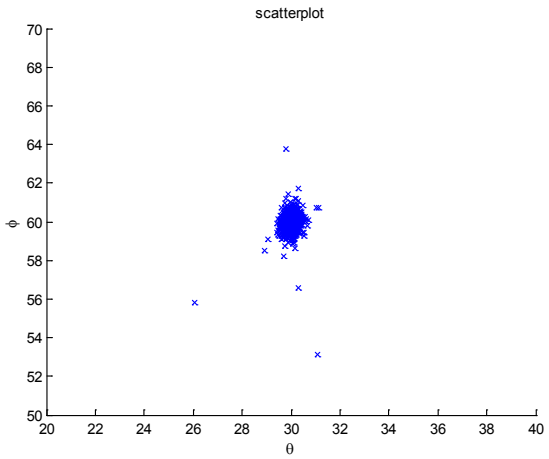

(b)

Figure 6 Scatter Plots Based on 1000 Independent Simulations

Increasing the number of temporal averaging improves DOA performance. Figure 7 shows the estimated angle error as a function of the number of snapshots N using a 19 element honeycomb array. Increasing the number of temporal averaging improves the matrix element estimation; consequently the estimated angle error is reduced. The 19 element array provides sufficient spatial smoothing in matrix element estimation. The estimated angle error after spatial smoothing is considerably smaller than the estimated angle error without spatial smoothing. After spatial smoothing, temporal averaging over 200 snapshots provides a very good estimation. Further increasing the number of snapshots does not significantly reduce the estimation error.

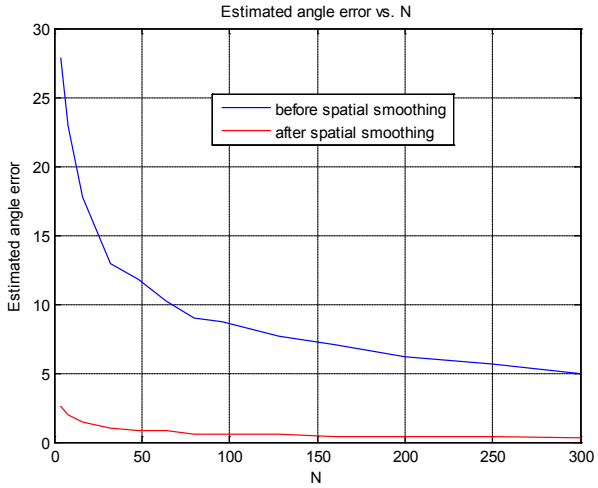

Figure 7 Estimated Angle Error as a Function of the Number of Temporal Averaging N

Better SNR help improves the DOA performance. Figure 8 shows the estimated angle error using 19 element honeycomb array with N = 32.

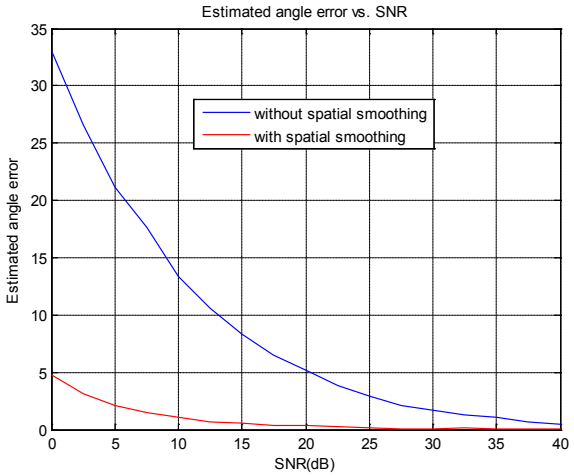

Figure 8 Estimated Angle Error as Function of SNR

With the elevation angle fixed at $\theta = 30^{o}$, Figure 9 shows that the estimation error is fairly independent of the azimuth angle. This result is based on using a 19 element array with SNR = 10 dB and temporal averaging over 32 snapshots; all matrices are 4×4. Figure 9 also indicates that the estimation error can be reduced by an order of magnitude if the elements of matrix r_{ij} are estimated by spatial smoothing and temporal averaging methods.

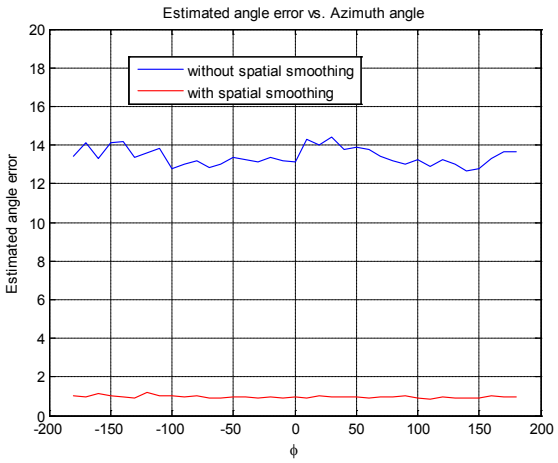

Figure 9 Estimated Angle Error as a Function of Elevation and Azimuth Angles

At high elevation angle, there are some special azimuth angles that yield a very large estimated angle error. The estimated angle error as a function of azimuth angle for a 9 element array for a signal impinging the array at high elevation angle ($\theta = 89^o$) is shown in Figure 10. This result is based on SNR = 10 dB and matrix elements are estimated by temporal averaging over 32 snapshots and spatial smoothing. For the signal impinging the 9 element array from azimuth angles of 0^o, 90^o, 180^o and 270^o, the estimated angle error is very large. This is due to the fact that the received signal vectors of subset (1, 2, 4, 5) and subset (2, 3, 5, 6) are very close if the signal impinging the array is from 90^o or 270^o. The received signal vector of subset (1, 2, 4, 5) and subset (4, 5, 7, 8) are very close if the signal impinging the array from 0^o or 180^o. The 9 element array produces very large estimation error whenever the signal impinging the array is from those special azimuth angles. Similarly, if a 19 element array is used to estimate signal's DOA, using the subset (1, 2, 4, 5) and shifting this subset to (2, 3, 5, 6) and (4, 5, 8, 9), it gives a large estimated angle error for the signal impinging the array at 90^o, 270^o, 150^o and 330^o.

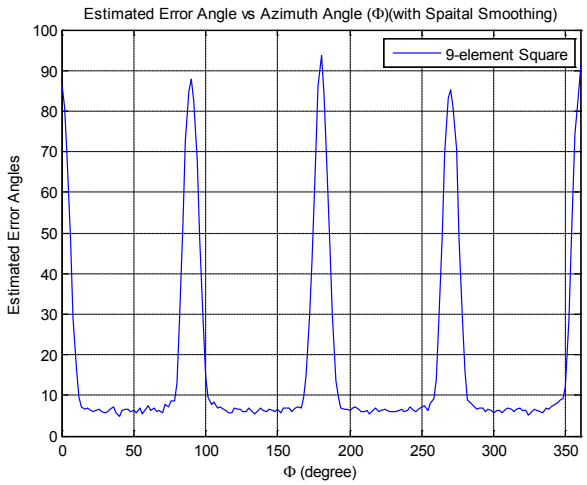

Figure 10 Estimated Angle Error vs Azimuth Angle for Elevation Angle $\theta = 89^o$

Matrix element r_{ij} is computed from the received data y(n) where the estimated DOA angles from Equations 22 and 23 assume the precise element position. Thus, whenever the array element position deviates from the ideal position, it degrades the accuracy of the estimation. The deviation of each array element position is assumed to be Gaussian with a standard deviation of δd where δ represents the percentage of inter-element spacing d.

Assume a tone signal impinging the array from azimuth angle $\phi = 60°$, and elevation angle $\theta = 30°$. The signal to noise ratio SNR = 10 dB. Using a 9 element square array and 4 element subarray, assume the percentage standard deviation of element position is $\delta = 2\%$, Figure 11 shows the scatter plot of the estimated DOA. The result of this scatter plot is obtained by testing over 100 different antennas; each antenna is simulated with 30 independent runs. The matrix element is estimated based on temporal averaging over 32 snapshots. Figure 11(a) shows the scatter plot without spatial smoothing and Figure 11(b) is the scatter plot with spatial smoothing. As shown in this figure, spatial smoothing tends to average out the effect of element position deviation. Consequently, the estimated signal's DOA is heavily concentrated on the ideal signal point (30°, 60°).

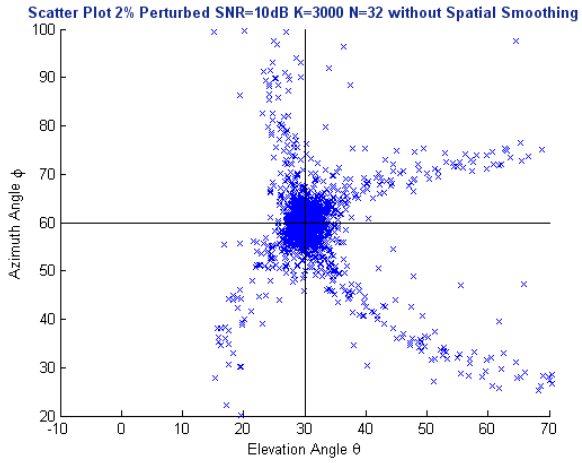

(a)

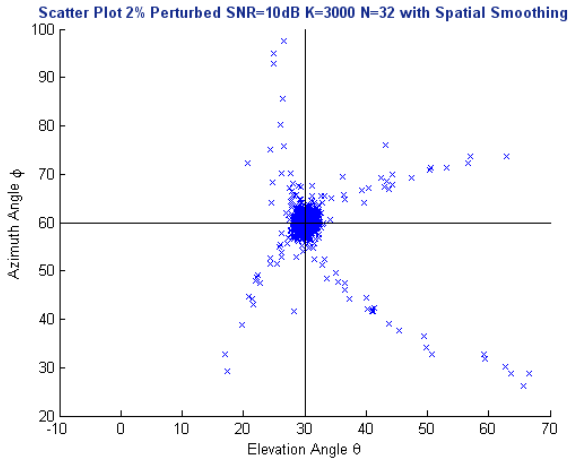

(b)

Figure 11 - Scatter Plots Based on 3000 Independent Simulations

The estimated angle error as a function of SNR is shown in Figure 12. This Figure shows that as SNR improves, estimation error decreases. In estimating matrix element r_{ij} without spatial smoothing, the estimation error could be considerably larger than the ideal case (with all elements in perfect position). Increasing the percentage standard deviation of element position to 5% results in a quite large

estimation even in a high SNR environment as shown in Figure 12(a). With the spatial smoothing, the estimation angle error is very close to the ideal case even when the percentage standard deviation of position error is 5%, as shown in Figure 12(b).

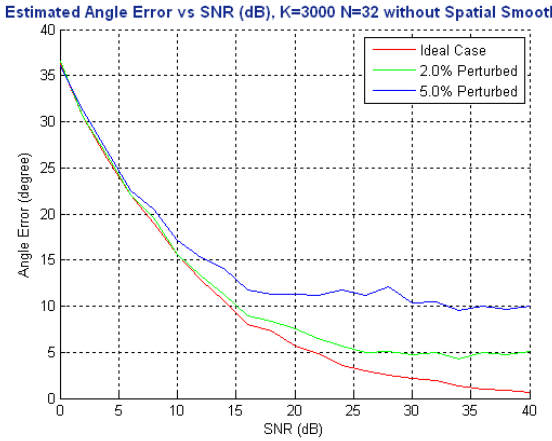

(a)

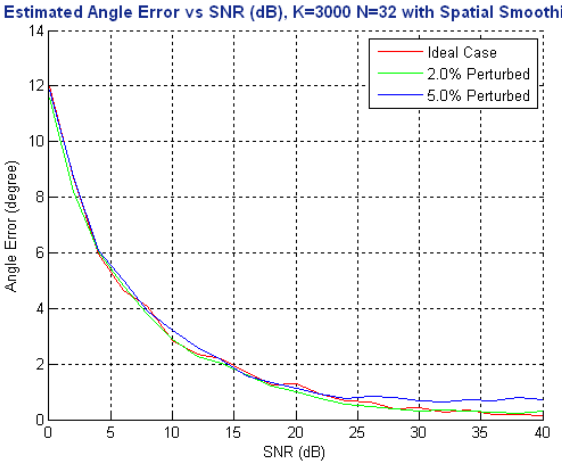

(b)

Figure 12 - Estimated Angle Error vs SNR

Increasing the number of temporal averagings improves the estimation accuracy. Figure 13 shows the estimated angle error as a function of the number of temporal averagings. This simulation is based on SNR = 10 dB with a 9 element square array. Matrix element r_{ij} is estimated by the temporal averaging and spatial smoothing method. This figure shows that the performance of the array with element position perturbation is very close to the ideal array case if the matrix element r_{ij} is estimated by the temporal averaging and spatial smoothing method.

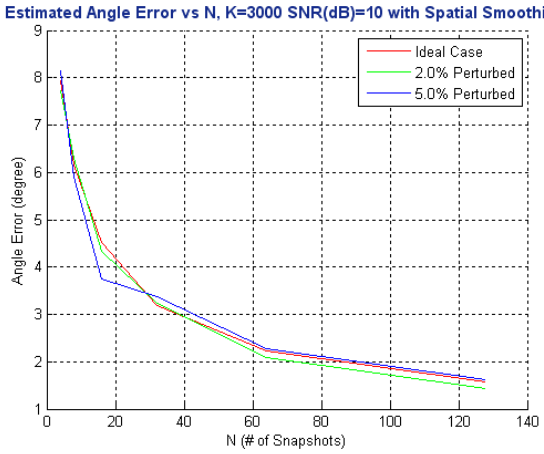

Figure 13 - Estimated Angle Error vs Number of Temporal Averaging

Using the 19 element honeycomb array and 4 element subarray, with the same SNR = 10 dB, the scatter plots of a non-ideal array with percentage element position standard deviations = 2% and 5% are shown in Figure 14(a), 14(b) respectively. The estimated matrix element r_{ij} is obtained by temporal averaging over 32 snapshots using the spatial smoothing method. If we compare Figure 14 with Figure 11, increasing the number of element reduces the estimation variance.

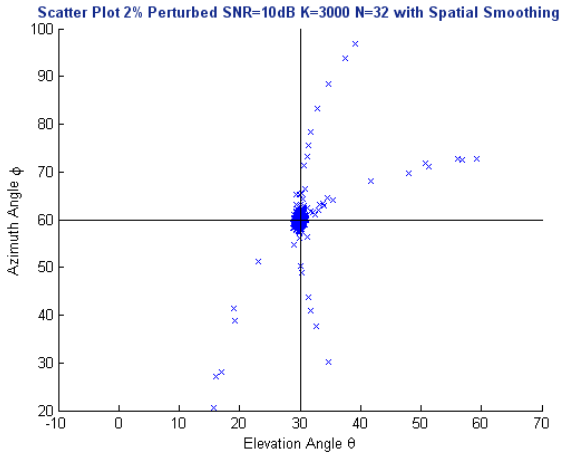

(a)

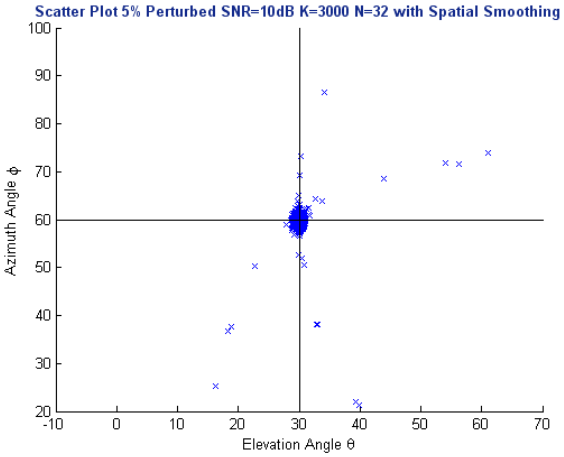

(b)

Figure 14 - Scatter Plot with Percentage Element Position Standard Deviation (a) $\delta = 2\%$ and (b) $\delta = 5\%$

The estimated angle error as a function of SNR is shown in Figure 7. The matrix element r_{ij} in Figure 15(a) is obtained by temporal averaging over 32 snapshots only. The matrix element r_{ij} in Figure 15(b) is obtained by temporal averaging over 32 snapshots and using spatial smoothing.

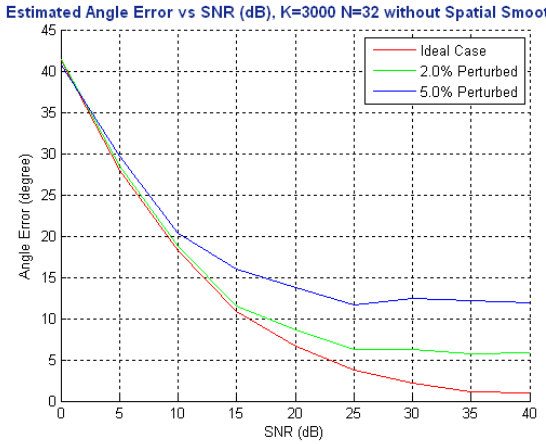

(a)

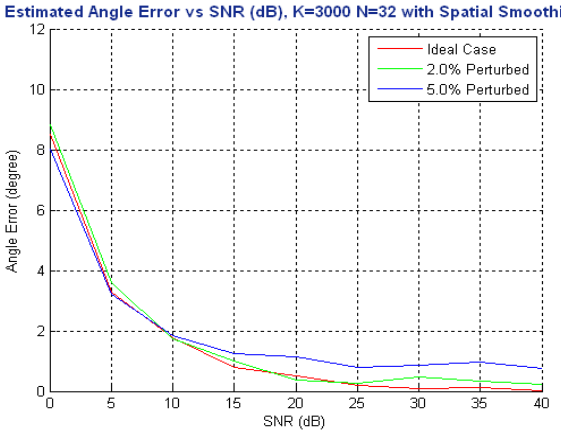

(b)

Figure 15 - Estimated Angle Error vs SNR

Increasing the number of temporal averagings improves the estimation accuracy. Figure 16 shows the estimated angle error as a function of the number of temporal averagings. This simulation is based on SNR = 10 dB with a 19 element honeycomb array. Matrix element r_{ij} is estimated by the temporal averaging and spatial smoothing method. This Figure shows that the performance of an array with element position perturbation is very close to the ideal array case if the matrix element r_{ij} is estimated by the temporal averaging and spatial smoothing method. Since this array has 19 elements, it provides an improved spatial smoothing. Compared to the 9 element square array (shown in Figure 12), the 19 element honeycomb array yields a smaller estimated angle error.

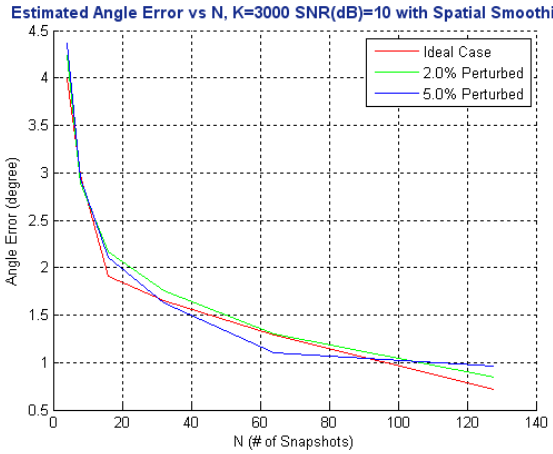

Figure 16 - Estimated Angle Error vs Number of Temporal Averaging

VI. Conclusion

The conclusions based on the results of this simulation study are summarized as follows:

1. The ESPRIT method estimates signal DOA by finding the roots of two independent equations closest to the unit circle. This method does not require using a scan vector to scan over all possible directions like the MUSIC algorithm. Compared with the MUSIC algorithm, the ESPRIT method obtains the DOA information by solving the simultaneous equations. This method reduces the processing requirements. It also sacrifices performance.
2. Estimation error is relatively independent of signal azimuth angle if the signal impinging the array is from a low elevation angle.
3. When the signal impinging the array is from high elevation angle, there are some critical azimuths angles that yield a very large estimation error. This is due to the fact that at those critical azimuth angles, the received data vectors are very close. Thus there is not sufficient information to process the received data. To avoid large estimation error, we suggest to alternatively choosing a different subset and shifting the subset in different directions.
4. Estimation error can be reduced by (a) using an array containing a large number of elements, (b) increasing the number of temporal averagings in matrix element estimation.
5. If the array element position deviates from the ideal position, DOA performance is degraded. However, spatial smoothing tends to average out the undesirable effect of random element position error. Whenever the matrix elements r_{ij} are estimated by the temporal averaging and spatial smoothing method, the estimated angle error is very close to the ideal case.
6. Increasing the number of array elements provides an improved estimation of matrix element r_{ij} by better spatial smoothing. Thus the estimated angle error of a 19 element honeycomb array is smaller than the corresponding estimated angle error of a 9 element square array.
7. If the signal impinges on the array from some special angles, shifting the subarray may not provide sufficient phase information. Consequently, the resulting estimated angle error can be quite large. In this case, we may have

to choose a different subarray and shift the subarray in a completely different direction. Detailed analysis is proposed in the future.

ACKNOWLEDGMENT

The authors would like to thank the Raytheon Space and Airborne Systems for its support of this investigation.

REFERENCES

[1] J. Proakis, D. K. Manolakis *Digital Signal Processing*, Prentice Hall, 2006, 4th Ed

[2] R.O Schmidt, "Multiple Emitter Location and Signal Parameter Estimation," *IEEE Trans. Antennas Propagation*, Vol. AP-34, 1986, pp. 276-280

[3] M. Pesivento, A. B. Gershman, M. Haardt, "A Theoretical and Experimental Study of a Root MUSIC Algorithm based on a Real Valued Eigen decomposition" Acoustics, Speech, and Signal Processing, 2000 Vol 5, pp 3049-3052

[4] Z. Aliyazicioglu, H. K. Hwang, M. Grice, A. Yakovlev, "Sensitivity Analysis for Direction of Arrival Estimation using a Root-MUSIC Algorithm" *Engineering Letters*, 16:3, EL_16_3_13

[5] G. F. Hatke, K. W. Forsythe, "A class of polynomial rooting algorithms for joint azimuth/elevation estimation using multidimensional arrays" *Signals, Systems and Computers*, 1994. 1994 Conference Record of the Twenty-Eighth Asilomar Conference, pp. 694 - 699 vol.1

[6] Z. Aliyazicioglu, H. K. Hwang, "Performance Analysis for DOA Estimation using the PRIME Algorithm" *10th International Conference on Signal and Image Processing*, 2008

[7] R. Roy, T. Kailath, **"**ESPRIT-estimation of signal parameters via rotational invariance techniques**"** *IEEE Transactions on Acoustics, Speech and Signal Processing*, 1989 , Vol. 37, pp.984 – 995.

[8] R. H. Roy, "ESPRIT-Estimation of Signal Parameters via Rotational Invariance Techniques," Ph.D. Dissertation, Stanford Univ., 1987.

[9] A. Swindlehurst and T. Kailath, "Azimuth/elevation direction finding using regular array geometries," *IEEE Trans. Aerospace Elect. Syst.*, vol.29, no. 1, pp. 145–155, Jan. 1993.

[10] R. Roy, A. Paulraj, and T. Kailath, "Estimation of signal parameters via rotational invariance techniques—ESPRIT," in *Proc. IEEE ICASSP*, vol.4, Tokyo, Japan, 1986, pp. 2495–2498

[11] R. Roy and T. Kailath, "ESPRIT—Estimation of signal parameters via rotational invariance techniques," *Opt. Engineering*, vol. 29, no. 4, pp.296–313, Apr. 1990.

[12] J. Bermudez, R. C. Chin, P. Davoodian, A. T. Yin Lok, Z. Aliyazicioglu, H. K. Hwang," Simulation Study on DOA Estimation using ESPRIT Algorithm" WCECS 2009, San Francisco, CA, 20-22 October, 2009.

[13] S. Haykin, "Adaptive Filter Theory, Prentic Hall, 2002, 4th Ed"